IEEE Access
Multidisciplinary ⋮ Rapid Review ⋮ Open Access Journal

Received 25 October 2023, accepted 28 November 2023, date of publication 1 December 2023,
date of current version 13 December 2023.

Digital Object Identifier 10.1109/ACCESS.2023.3339127

RESEARCH ARTICLE

Quantum Mechanism-Based Convolution Model for the Classification of Pathogenic Bacteria

ISRA NAZ[1], JAMAL HUSSAIN SHAH[1], MUHAMMAD HABIB UR REHMAN[1], (Senior Member, IEEE), MUHAMMAD RAFIQ[2], (Member, IEEE), AND GYU SANG CHOI[3], (Member, IEEE)

[1]Department of Computer Science, COMSATS University Islamabad, Wah Campus, Islamabad 45550, Pakistan
[2]Department of Game Software, Keimyung University, Dalseo-gu, Daegu 42601, Republic of Korea
[3]Department of Information and Communication Engineering, Yeungnam University, Gyeongsan-si 38541, Republic of Korea

Corresponding authors: Gyu Sang Choi (castchoi@ynu.ac.kr) and Muhammad Rafiq (rafiq@kmu.ac.kr)

This work was supported in part by Basic Science Research Program through the National Research Foundation of Korea (NRF) funded by the Ministry of Education (NRF-2019R1A2C1006159), in part by the 2023 Yeungnam University Research Grant, and in part by the National Research Program for Universities (NRPU) Higher Education Commission (HEC) under Project ID 7794, COMSATS University Islamabad, Wah Campus.

ABSTRACT Water, especially drinking water, should be clean and free of disease-causing bacteria because of its critical role in life. However, it isn't easy to identify and classify them rapidly at an early stage. Primarily, the examination of water is performed manually to check the contamination level. Some researchers have proposed techniques to detect and classify bacteria images, but this field still needs more attention. In this research work, a robust Quantum Convolutional Neural Network (QCNN) classification model is proposed to classify the six major categories of pathogenic bacteria. For the acquisition of pathogen images, different slides are created through the gram-staining process, and then images are captured from those slides. DIBaS is the publicly available dataset that provides these slides captured through gram-staining, which is used to evaluate the proposed methodology. So, in the first step, database preprocessing, small patches are extracted from slide images. However, the extracted patches were not clear and very useful, so the Enhanced Super-Resolution Generative Adversarial Network Model (ESRGAN) was applied to images to improve the image quality of extracted patches. The third step is to extract the deep features and classify bacterial images using the QCNN model, in which the Quantum Convolutional layer is added, and classical data is converted into quantum data to perform classification. Based on the results of classification experiments using the QCNN model, the accuracy is 96.54%.

INDEX TERMS Generative adversarial network (GAN), pathogens, quantum convolutional network (QCNN), super resolution.

I. INTRODUCTION

Pathogen detection is an essential aspect of healthcare, as it allows medical professionals to identify and treat diseases caused by various pathogens rapidly. However, current methods of pathogen detection are often time-consuming and expensive. In the past decade, image-processing techniques have become increasingly popular in detecting pathogens. Image processing can detect pathogens' presence in a sample by analyzing their shape, size, color, and other features. Image processing also provides a means of quantifying the number of pathogens present in a sample. Recent advances in image processing techniques have enabled the detection of a wide range of pathogens with high accuracy. These techniques include machine learning algorithms, deep learning networks, and other image processing techniques [1]. Machine learning algorithms detect and classify pathogens based on their image features. Deep learning networks identify and classify pathogens based on their morphological features. Other image processing techniques, such as feature

The associate editor coordinating the review of this manuscript and approving it for publication was Easter Selvan Suviseshamuthu.

extraction, segmentation, and classification, are also used to detect pathogens. Recent studies have explored image-processing techniques to detect various pathogens, including viruses, bacteria, and fungi. Image processing techniques have enabled the development of highly accurate and efficient pathogen detection systems. These systems are used in various settings, including clinical laboratories, food safety laboratories, and agricultural settings. Image processing techniques have been used to develop rapid and cost-effective pathogen detection methods. In addition, image-processing techniques can detect pathogens in complex samples, such as those containing multiple species or those having a high concentration of pathogens [2]. Despite the advances in image processing techniques, several challenges still need to be addressed. These include the detection of low-level pathogens, the detection of pathogens in complex samples, and the development of accurate and efficient systems for pathogen detection. In addition, future research should focus on improving the accuracy of image processing techniques and developing more efficient algorithms for pathogen detection.

In this paper, we present a novel approach for pathogen detection using a Quantum convolutional neural network (QCNN) model. This approach is based on a combination of convolutional and recurrent neural networks and utilizes various image-processing techniques to classify the pathogen images. We evaluate the performance of this model on a dataset of pathogen-infected images and show that it outperforms existing pathogen detection methods. We also describe the model architecture and discuss its potential applications in the healthcare industry. The proposed methodology provides a comprehensive approach for pathogen classification, incorporating dataset preprocessing, super-resolution techniques, and the utilization of quantum computing in the classification model.

The significant contributions of the proposed methodology are as follows:

- The slides produced by Gram staining are clustered with numbers of pathogens, so image patches are extracted from slide images. Irrelevant patches are removed, the quality is enhanced, and the dataset is expanded for improved performance.
- The QCNN model is used to effectively classify pathogens after enhancement based on their distinct features, enhancing the accuracy of pathogen classification.
- It leverages the QCNN model for accurate classification of pathogenic bacteria, demonstrating its potential in improving pathogen identification and classification processes.

II. LITERATURE REVIEW

Different researchers have presented various techniques for the detection and classification of microorganisms. Some of the techniques are discussed in this section. Polymerase chain response (PCR) is one of the primary elective recognition techniques being tested. PCR has been demonstrated to be a fast, exceptionally touchy, and precise strategy. It has effectively been utilized tentatively to distinguish pathogenic infections, microorganisms, and protozoa in water and wastewater and set up strategies for pathogens identification [3]. Polymerase chain response (PCR), culture, state-considering strategies, and immunology-based techniques are the most widely recognized devices utilized to determine pathogens' location. They include DNA investigation, checking of microscopic organisms, and antigen–neutralizer communications separately.

A portion of the pathogens known to be sent through polluted drinking water leads to serious and now and again perilous sickness. Models incorporate typhoid, cholera, irresistible hepatitis (brought about by hepatitis an infection [HAV] or HEV), and illness brought about by Shigella spp. Detection and identification of the pathogen is essential, and multiple researchers present several methodologies for performing this task. Some of them are discussed in this section. In [4], the author used multiclass uphold vector machines (MC-SVM) to distinguish between Legionella species. The quickly recognizable proof of water pathogens is essential for controlling food quality. The framework for the quick and name-free distinguishing proof of bacteria depends on the guideline of laser dispersing from the bacterial organisms. The clinical model comprises three sections: the laser bar, photodetectors, and the information procurement framework. The bacterial testing test was blended with 10 mL of refined water and set inside the machine chamber. At the point when the bacterial organisms pass by the laser bar, the dissipating of light happens because of the variety in size, shape, and morphology. Because of this explanation, various sorts of microbes show their one-of-a-kind light-dispersing designs. The photograph locators were organized at the environmental factors of the example at multiple points to gather the dispersed light. The photodetectors convert the dissipated light power into a voltage waveform. Another researcher used the Maximum Relevance Minimum Redundancy (mRMR) and SVM classifier to highlight the order of three diverse bacterial organisms E. faecalis, E. coli, and S. aureus [5]. Vibrio class involves around 100 species, generally of the marine or freshwater root. In [6], the author provides an overview of Vibrio pathogens in rural water and how Vibrio pathogens are implicated in public health.

Clustering methods are also widely used for the detection of microorganisms. For example, [7] used an adaptive neighborhood similarity comparison algorithm to segment medical microorganisms (bacteria) from images of multicolored microbes with a complex, noisy background. References [8], [9], [10], [11], and [12] used K-mean clustering algorithms to segment TB bacilli from tissue images. In [13], the author utilized K-mean clustering to segment leishmania and used the Modified Fuzzy divergence algorithm to segment Plasmodium from low-contrast images. Reference [14] utilizes Self Organizing Map (SOM) to segment bacteria and measure the severity of the diseases. References [15], [16], and [17] also used clustering algorithms to segment a medical organism: TB bacilli. Clustering algorithms are also used

to segment water-borne microorganisms. For example, [18] used watershed algorithms for segmenting P. notatum water-borne organisms. Reference [19] segmented the water-borne bacteria using the K-mean clustering algorithm. Clustering algorithms are also used for the segmentation of Industrial bacteria [20], Environmental microorganisms [21], [22], and science microorganisms [23], [24], [25], [26].

Labs breaking down microbes are promptly onboarding sub-atomic advancements to help oversee irresistible sickness because of the squeezing need for instruments that encourage compelling dynamics, improve future results, and diminish care expenses. Applied Biosystems pathogens identification arrangements convey quick, exceptionally delicate tests that empower precise outcomes for the most well-known worldwide irresistible illnesses utilizing confirmed multiplex constant PCR innovation. Our adaptable substance syndromic boards let you test for numerous markers during the first run-through, making them a significant and expense-proficient approach for finding more solutions from your examples with expanded trust in your research facility.

To identify microorganisms present in water, different researchers used traditional methods like the random forest, SVM, Naïve Bayes, and decision tree. Reference [27] classify the bacterial images of the DIBas dataset using the method of SVM and Bag of Word (BOW) features. Similarly, [28], [29] also used the SVM classification method to classify bacteria. Reference [30] used decision tree algorithm and color, shape, size, and cluster shape as features for classification. It used only 400 images of the DIBaS dataset. Reference [31] used naïve Bayes algorithm and canny edge detection to classify bacteria in low training time.

The existence of noise and data uncertainty poses significant challenges that must be addressed from theoretical and computational perspectives. Robust optimization has become more significant as a modeling framework for mitigating parametric uncertainties, both in terms of theoretical and practical considerations [32]. For this, different researchers have proposed work for modeling real-life data in various application fields, even in the presence of parametric uncertainties. Reference [33] presents a novel nonparametric regression approach that utilizes multivariate adaptive regression splines, further enhanced by continuous optimization techniques. Compared to MARS, a nonparametric regression technique, the CMARS algorithm demonstrates superior accuracy, robustness, and stability. The study posits that CMARS might serve as a viable substitute for MARS. In [34], the authors present the resilient conic generalized partial linear model (RCGPLM) approach. This method integrates linear and nonlinear regression models to enhance accuracy and simplify complexity. The methodology is employed on an extensive dataset comprising 45 emerging markets from 1980 to 2005. A balance is struck between tractability and robustification to address limitations in computer power. The authors in [35] introduce a Robust Conic Generalized Partial Linear Model (RCGPLM) that utilizes the RCMARS approach to effectively distinguish between linear and nonlinear variables, allowing for distinct modeling of each variable type. The model is enhanced by the application of robust optimization techniques to address and mitigate the impact of uncertainties present in the data. The proposed methodology seeks to reduce the variability in estimation and may be utilized in both regression and classification scenarios. The RMARS approach, an enhanced version of the MARS technique that effectively addresses uncertainties associated with financial data, is proposed in [32]. The researchers investigated the topic of RMARS within the context of polyhedral uncertainty. A robust optimization strategy is employed to enhance the feasibility of the RMARS method, demonstrating its capacity to generate models with reduced variability in parameter estimations and accuracy measurements. The work proposed in [36] focuses on enhancing the robustness of the CMARS algorithm by including polyhedral uncertainty sets. The authors provide a novel technique known as RCMARS, which integrates uncertainty into the model by including complexity measures in the form of integrals of squared first- and second-order derivatives of the model functions. The outcomes of the sensitivity analysis conducted on the parameter estimations indicate that RCMARS yields superior accuracy compared to CMARS, as evidenced by the narrower confidence intervals seen on the variables.

Deep learning algorithms have proven to be an outstanding achievement in the processing and analysis of microscopic images. The different researchers used deep learning methods for the identification of bacteria. Reference [37] the CNN method based on 3D images was used to identify bacteria from the zebrafish dataset. References [38], [39], [40] used CNN, VGGNet, and Resnet 50, respectively, [41] used CNN, Alexnet, and autoencoder to identify bacteria from the dataset of Peking University First Hospital. Reference [42] applied a CNN model, ''Xception architecture'' for identifying bacteria from a public database, and the CNN model was based on transfer learning. Reference [43] used a Densely Connected Convolution Network to identify bacteria of three classes. References [28], [44], and [45] used CNN to detect bacteria from images.

Quantum-based technologies known as Quantum Computing (QC) are growing rapidly, driven by the interplay between government, academia, startups, and multinational companies such as Microsoft, Google, and IBM. Quantum Machine Learning (QML) based systems, including quantum classification and detection models, attract many researchers. Moreover, quantum computers are also entering an early industrial era. In QML, hybrid quantum circuits (HQC) include quantum states, superposition, and amplitude encoding, providing a quantifiable edge in classification tasks relevant to image processing. Using QML algorithms, pathogen image data is used to classify it through HQC. By comparing with classical data processing, it shows that the HQC can enhance the speed and accuracy of the classifier model [46]. A comparison of some methodologies discussed in this section is provided in Table 1 below:

TABLE 1. Comparison of some existing methodologies for bacteria images.

Ref.	Dataset	Methodology	Purpose
[7]	Medical microorganisms	Adaptive neighborhood similarity comparison algorithm for bacterial segmentation	Segmentation
[8]	TB bacilli	K-means clustering algorithm for TB bacilli segmentation	Segmentation
[13]	Leishmania	K-means clustering for Leishmania segmentation; Modified Fuzzy divergence algorithm for Plasmodium segmentation	Segmentation
[14]	Bacteria	Self-Organizing Map (SOM) for bacteria segmentation and disease severity measurement	Segmentation
[15]	TB bacilli	Clustering algorithms for TB bacilli segmentation	Segmentation
[17]	P. notatum water-borne organisms	Watershed algorithm for segmenting P. notatum water-borne organisms	Segmentation
[19]	Water-borne bacteria	K-means clustering algorithm for water-borne bacteria segmentation	Segmentation
[20]	Industrial bacteria	Clustering algorithm for industrial bacteria segmentation	Segmentation
[23]	Environmental and science microorganisms	Clustering algorithms for environmental and science microorganism segmentation	Segmentation
[27]	DIBas dataset	SVM and Bag of Word (BOW) features for bacterial image classification	Classification
[30]	DIBaS dataset	Decision tree algorithm and various features for bacterial classification	Classification
[32]	Zebrafish dataset	CNN based on 3D images for bacterial identification	identification
[36]	Peking University First Hospital dataset	CNN, Alexnet, and autoencoder for bacterial identification	identification
[37]	Public database	CNN model based on transfer learning (Xception architecture) for bacterial identification	identification

III. PROPOSED METHODOLOGY

In this research work, the QCNN model is used to classify different pathogens of water bacteria. The proposed methodology consists of multiple steps: Dataset pre-processing, super-resolution for obtaining high resolution from low-resolution images and categorizing distinct kinds of bacteria. Pathogens images dataset is in the form of slide images; therefore, small image patches are extracted from those slides, but these patches were blurred and were not of high quality, so those small images were passed to the Enhanced Super-Resolution Generative Adversarial Network Model (ESRGAN), where this model converts the low-resolution images into higher resolution images. The QCNN model was prepared to separate conventional highlights to group microbes. For the classification of 6 categories, cell images are passed to the QCNN model in the testing phase. The proposed methodology for pathogen classification is graphically represented in Figure 1. The detailed description of each phase of the proposed solution is described in the sections below.

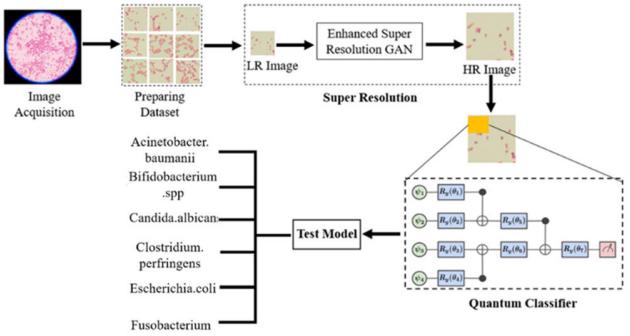

FIGURE 1. Flow diagram of proposed work.

A. DATASET PREPROCESSING

Data preparation is a vital stage in machine learning that enhances data quality and makes extracting valuable insights from the data easy. The experimentation is performed on the DIBaS image dataset. Pathogen images of the DIBaS dataset are slide images, so preprocessing is performed on the dataset. Slides or bacterial images are produced mainly by Gram staining and light microscopy of the freshly grown cultures. The slides are prepared by adding a small amount (with the help of a wire loop) of culture and suspending the bacterial cells in a drop of distilled water. Then, bacteria are heat-fixed on the glass slide after drying the smear. Crystal violet is added to the smear and washed with water after 1 minute. Gram's Iodine is added and washed with water after 1 minute and then rinsed with ethanol (70%). Then, the slide is washed immediately with plenty of water to remove excessive amounts of ethanol. Safranin is added to the smear and washed with water after 1 minute. The slides are air-dried, and a drop of immersion oil is added to the smear. The images of bacteria are observed at least on 100X magnification using camera camera-fitted Light microscope. The bacteria are then identified by using the developed software. Some of the images of the dataset are shown in Figure 2. The details of the DIBaS dataset used for experimental evaluation are shown in Figure 3.

Data preprocessing is used in Machine Learning to clean and organize raw data, making the creation and training process easier and more appropriate for the Machine Learning models. In this step, images obtained through the gram staining process are divided into multiple patches, and the useless patches (not having bacteria in them) are removed from the dataset. Figure 4 illustrates the visual representation of the patch generation process from the slide images.

Image preprocessing is additionally applied to the restricted size of the dataset to build the size of the dataset to perform well for the huge size of the dataset. DIABs dataset

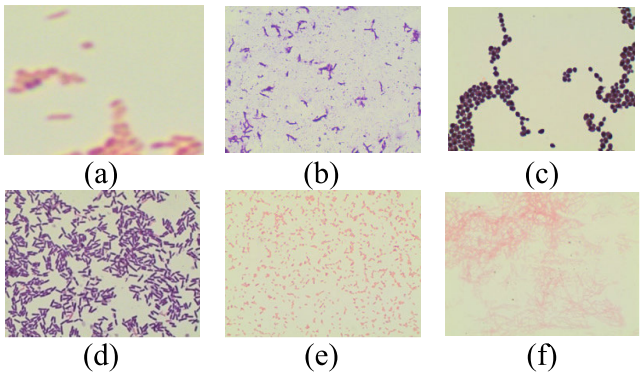

FIGURE 2. DIBaS Dataset Images: (a) Acinetobacter.baumanii(Ai) (b) Bifidobacterium.spp(Bp) (c) Candida.Albicans(Ca) (d) Clostridium.perfringens(Cp) (e) Escherichia.Coli (Ei) (f) Fusobacterium(Fm).

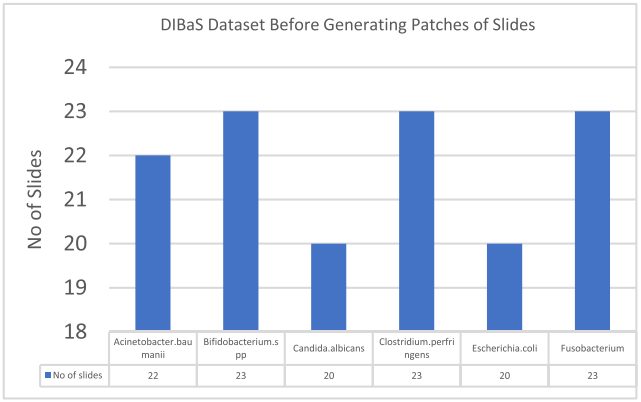

FIGURE 3. Details of DIBaS dataset before generating patches of slides.

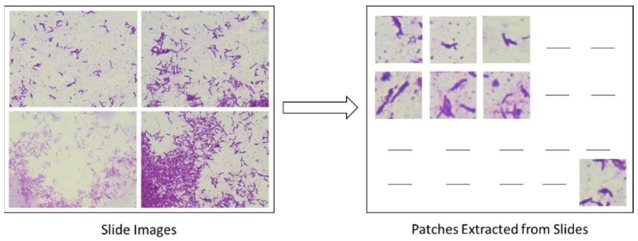

FIGURE 4. Patch Generation for Escherichia. Coli images.

has six classes, each containing a minimum of 20 slides. In this phase, the size of the DIABs dataset is expanded to at least 1080 images in a single class. Another reason for this step is to ensure that every classification of microbes has the same number of tests.

B. SUPER RESOLUTION

The Super-resolution technique generates high-resolution images from a single image or multiple low-resolution images. Super-resolution enhances the resolution and quality of an image. This is used as the preprocessing step, as the patches were extracted from slides to form a pathogen dataset. But those patches were not clear, and the quality of the images was also deficient. The slides generated through gram staining are clustered with numbers of pathogens, so as a first preprocessing step, the slides are divided into multiple patches. Almost 55 patches are extracted from each slide, which are of very low resolution and small in size. So, the Enhanced Super Resolution Generative Adversarial Network model is applied to improve the quality of the patches extracted from different slide images.

C. CLASSIFICATION MODEL

The QCNN model was prepared to separate six categories of pathogenic bacteria for the classification. This section systematically discusses the detailed mathematical representation of the QCNN model.

1) QUANTUM CLASSIFICATION BACKGROUND

In quantum computing, a quantum state or superposition of qubits is often represented by the "|" (pipe symbol) followed by ">" (greater than sign), known as a ket notation. A quantum system's state is denoted by a vector called a ket. The "|" sign indicates the ket's beginning, and its completion by the ">" symbol. Then, the ket defines the quantum states (or qubits). Traditional Machine Classification problems can be represented as $CPs = cp1, cp2, \ldots, cpn$ where CPs is a list of target classes and a set of training-data as $D_n = (x_1, y_1), \ldots, (x_i, y_i), \ldots, (x_n, y_n)\}$ where x_i represented as features (f_n), of data-point $dp_{(i)}$ properties and y_i is the correspondence of that $dp_{(i)}s$. For solving classification problems of the QML domain, first, classical data is converted to quantum data (qd), and in training samples that qd is represented as $D_n = (|\psi_1\rangle, y_1), \ldots, (|\psi_i\rangle, y_i), \ldots, (|\psi_n\rangle, y_n)\}$ where $|\psi_i\rangle$ is the i^{th} order of the quantum state(qs) of D_n, $|\psi_i\rangle \epsilon C^{2^d}$ and for the classification of multiple classes $y_i = cp1, cp2, \ldots, cpn$ where $x_i \epsilon \mathbb{R}^d$ and d are real-valued attributes., there are several methods used for the mapping of classical data to quantum data, like amplitude-encoding and basis-encoding.

Basis Encoding (BE) is the most straightforward technique used for encoding classical data into quantum data. BE acquaintances between the computational of n-qubit input and n-bit classical inputs, In classical input (1100), the string is encoded to 4 qubits ($|1100\rangle$) in quantum states. The representation of the data in computational states of qubits is as follows:

$$|D\rangle = \frac{1}{\sqrt{N}} \sum_{n=1}^{N} |X^n\rangle \tag{1}$$

where $D = X_1, X_2, \ldots, X_P N$ is classical data from a binary string, $X^n = a1, a2, a3 \ldots aX$, $ai \in 1, 0$ And i $\in \{1, 2, \ldots, k\}$ and k is number of features. Amplitude Encoding (AE) is another popular technique used in encoding for QML algorithms. The idea behind amplitude encoding is constructed on the association between classical data and quantum state amplitudes (QSA). For encoding of classical data vector to quantum amplitudes, the first phase is to normalize the classical-data vector and passed it through

quantum state amplitudes [44], [45].

$$X = \begin{bmatrix} x_1 \\ x_2 \\ . \\ . \\ x_{2^n} \end{bmatrix} \tag{2}$$

where normalized vector denotes as X, $x \in$ superscripted C represents complex numbers. QSA can be encoded, as you can see in the below equation:

$$|\psi_x\rangle = \sum_{i=1}^{2^n-1} x_i \, |\mathrm{i}\rangle \tag{3}$$

where $\psi \in \upsilon$ is used as quantum amplitude, this quantum amplitude is described in the following section III-C3.

Variational quantum circuits (VQC) are parameterized quantum circuits (QC). In QML, most of the hybrid quantum algorithms rely on quantum-based circuits (QBC). The construction behind the variation in QBC is to optimize parameters according to their objective functions. Modified QBC consists of 3 major phases; in phase one, a classical normalized vector is passed to quantum amplitudes, in the second phase, which can also be called the quantum phase, and then again is the classical phase. Phase two state preparation is performed; QBC is the backbone of the modified circuits that parameterizes the input (X) according to the number of parameters and measurements. The third phase comprises the QBC output and the learning algorithm's objective function. QBC uses in various fields of machine learning [48], [49], optimization [50], and deep learning [51].

2) QCNN CLASSIFICATION MODEL

Quantum convolution neural networks (QCNNs) used in the proposed methodology is uses quantum computing to improve the accuracy of image processing tasks. The classification process for this QCNN model follows a similar structure to that of classical convolutional neural networks (CNNs) but uses quantum computing to speed up the process and improve accuracy. There are several concepts that are used in our research: 1) Quantum-circuit to handle q-bits known as Bloch-Spere, 2) Quantum Fourier Transform (QFT) to convert classical image data into higher-dimension images known as quantum-based images (QBI), 3) Quantum Convolutional Layers embedding the Neural Network model to extract quantum-based features, and 4) Quantum Entanglement and Superposition used in quantum circuits to categories the pathogen images. The classification process of a QCNN starts with a quantum circuit that takes a microscopic pathogen image as input and applies a set of quantum operations to generate a quantum feature vector. This feature vector is then used to classify the input image into six categories of pathogens. Our QCNN model uses a combination of quantum concepts and deep learning to perform classification tasks which are: 1) Quantum Fourier Transform (QFT): used to map the input data into a higher-dimensional feature space, 2) Variational Quantum Eigensolver (VQE): used to find the optimal weights for the network, 3) Quantum Approximate Optimization Algorithm (QAOA): used to optimize the weights for the network, and 4) Measurement-based classifier: used to classify the data into its respective classes of the pathogen.

TABLE 2. Parameters of model.

Parameter Name	Value
Number of Q-Bits	08
Learning rate	0.0004
Batch-size	04
Number of V-layers	06
Q-weight	0.01
Max-Epochs	20

For classification, the QCCN model used six variational layers and a batch size of 4, which means four samples are used for each training step. The parameters which are used for the proposed model are shown in Table 2. QCNN network has eight quantum bits with the initial spread of random quantum weights of 0.01 and a learning rate of 0.0004 per step with the reduction applied after every ten epochs in learning rate of gamma_lr_scheduler = 0.1. The quantum pooling layers and quantum fully connected layers are used, which are described in the following section.

3) TRAINING MODEL

This section will first describe the basics of QC. Like a classical bit(Cb), a quantum bit(Qb) known as qubits represented as $(|0\rangle, |1\rangle)\rangle$, these qubits are used in a superposition state $\alpha\,|0\rangle + \beta|1\rangle$ with amplitudes

$(\alpha, \beta) \epsilon C$ as $|\alpha|^2 + |\beta|^2 = 1$. With n no. of qubits, 2^n superposition binary combinations are possible, each with a specific amplitude. The i^{th} combination like., $|01 \ldots 110\rangle$ is represented as $(|i\rangle)$, where the vector is represented as v, $v \epsilon \mathbb{R}^d$ encoded with a quantum state that includes qubits $\lceil \log(d) \rceil$. This type of encoding works as quantum superposition and for the components, $(\upsilon 1, \cdots, \upsilon d)$ where υ used as the amplitudes of the d binary combinations. This state is defined as:

$$|\upsilon i\rangle := (\frac{1}{\|\upsilon\|}) \sum i \in [d] \upsilon i |i\rangle \tag{4}$$

where $|i\upsilon$ a register denotes the i^{th} vector. QC starts working by applying quantum gates, and these are defined by unitary matrices acting on one to two qubits, e.g., the Hadamard-gate that maps:

$$|0\rangle \, 7 \rightarrow 1\sqrt{2}(|0\rangle + |1\rangle) \tag{5}$$

and

$$|1\rangle \, 7 \rightarrow 1\sqrt{2}(|0\rangle - |1\rangle) \tag{6}$$

The output is the quantum state that is used to measure the classical data. The qubit output is represented as $(|0\rangle + \beta|1\,|0\rangle)$ yields either 1 or 0, with the highest probability equal to the $(\text{amplitude})^2$. The details of the QCNN model used in our proposed system are shown in Figure 5.

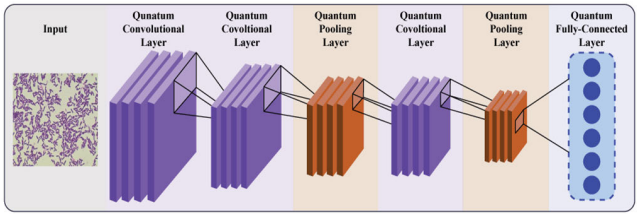

FIGURE 5. Details of the QCNN model.

a: QUANTUM CONVOLUTION LAYER

Let X^{l} is the input pathogen image, and K^{l} denoted as a kernel, and it for *layer*(l) of a CNN, and f it's a real number $f : \mathbb{R} \to [0, C]$ where C should be greater than $0(C > 0)$ for nonlinear function so that $f(X^{\mathrm{l}} + 1) := f(X^{\mathrm{l}} * K^{\mathrm{l}})$ is the output for l. Given that X^{l} and K^{l} saved in Quantum Random Access Memory (QRAM), for the quantum-based algorithm, the precision parameters represented as ε and η both should be greater than $0(\varepsilon > 0 \; and \; \eta > 0)$, to create quantum state $|f(\bar{X}^{\mathrm{l}} + 1)\langle$ such that $|f(\bar{X}^{\mathrm{l}} + 1) - |f(X^{\mathrm{l}} + 1)\|\infty \leq 2\varepsilon$ and to retrieve classical-tensors $X^{\mathrm{l}} + 1$ and for each pixel i.

$$\mathrm{f}(X_i^{\mathrm{l}+1}) \text{ represented as CXL} \tag{7}$$

$$\mathrm{f}(\bar{X}_i^{\mathrm{l}+1}) \text{ represented as QXL} \tag{8}$$

$$\begin{cases} \left|X_i^{\mathrm{l}+1} - \mathrm{CXL}\right| \leq 2\varepsilon \to \&QXL \geq \eta \\ X_i^{\mathrm{l}+1} = 0 \to \&\mathrm{QXL} < \eta \end{cases} \tag{9}$$

The running time of the Quantum algorithm is $\tilde{O}\left(\frac{1}{\varepsilon\eta^2} \cdot \frac{M\sqrt{C}}{\sqrt{\mathrm{E}\left(\mathrm{f}(\bar{X}\mathrm{l}+1)\right)}}\right)$ where E(·) represents the average value, $\tilde{O}$ is used to hide the factors polylogarithmic in the size of X^{l} and K^{l}, the parameter $M = max_{p,q}\|A_p\|\|F_q\|$. The maximum product M of norms from X^{l} and K^{l} subregions. The no of elements in the X^{l} (input) and K^{l} (kernels) appear with a polylogarithmic contribution in the running time. The main advantage of this algorithm is that it helps us to use it with larger and deeper kernels. There are no elements involved in the input hidden in the precision parameter η in the running time.

b: QUANTUM POOLING LAYER

After the convolutional layer, the pooling layer is added whose job is to reduce the spatial size of the representation to bring the total number of parameters under control. In our model, we use an approach called "average pooling," which determines the pooling layers by calculating the average value for each patch on the feature map. Consider a pixel pooling operation that is applied with a stride of 2 pixels and has a size of 2 × 2 pixels. It is possible to directly actualize it by disregarding the final qubit in the quantum environment as well as the mth qubit. The input image $|X^{l} = (x_1^{\mathrm{l}}, x_2^{\mathrm{l}}, x_3^{\mathrm{l}}, x_4^{\mathrm{l}}, \ldots, \ldots, x_{M^2}^{\mathrm{l}})^T$ after this operation can be expressed as the output image |Op which is equal to (10), as shown at the bottom of the page.

c: QUANTUM FULLY CONNECTED LAYER

The data that was retrieved by the layers that came before it is compiled by fully connected layers to generate the final output, which is then inserted at the very end of the QCNN model. We refer to the quantum fully connected layer as a parametrized Hamiltonian that is up to a seconder order correlation in correlation. This Hamiltonian $(\mathcal{H})$ c onsists of identity operators I and Pauli operators σ_z,

$$\mathcal{H} = h^0 \mathrm{l} + \sum_i h^i \sigma_z^i + \sum_{i,j} h^{ij} \sigma_z^i \sigma_z^j \tag{11}$$

where h^0, h^i, h^{ij} are the parameters, and Roman indices i, and j denote the qubit on which the operator acts, i.e., σ_z^i means Pauli matrix σ_z acting on a qubit at site i. The parameters in the Hamiltonian matrix $\mathcal{H}$ are updated by the gradient descent method.

IV. RESULTS AND DISCUSSION

For the classification of discriminatory types of pathogens, the experimentation is performed on a pathogen dataset having six classes of pathogens: Acinetobacter.baumanii (Ai), Bifidobacterium.spp (Bp), Candida.Albicans (Ca), Clostridium.perfringens (Cp), Escherichia.Coli (Ei), and Fusobacterium (Fm). These images are tested on Quantum Convolutional Neural Network (QCNN) based classifier. All the steps of the proposed algorithms are implemented in Python using an operating system of 64 bits with 16GB RAM, a 3.6GHz processor, and NVIDIA 4GB 1660 GTX. For the evaluation of the proposed methodology, performance measures of accuracy, specificity, precision, Recall, and F1 score are used.

The results of the pathogen classification achieved by the proposed work are discussed in this section. Firstly, low-resolution pathogen images are converted to high-resolution images through the ESRGAN model. In this proses the images are enlarged and their resolution is enhanced. Some of the pathogen images are shown in Figure 6.

For the evaluation purpose, images are also tested using a basic CNN model having 4 Convolutional layers, 5 dropout layers, and 2 max-pooling layers. The results of pathogens

$$\left(\frac{\sqrt{\mathrm{Xl}_1^2 + \mathrm{Xl}_2^2 + \mathrm{Xl}_{M+1}^2 + \mathrm{Xl}_{M+2}^2}, \sqrt{\mathrm{Xl}_3^2 + \mathrm{Xl}_4^2 + \mathrm{Xl}_{M+3}^2 + \mathrm{Xl}_{M+4}^2}, \ldots,}{\sqrt{\mathrm{Xl}_{M^2-M-1}^2 + \mathrm{Xl}_{M^2-M}^2 + \mathrm{Xl}_{M^2-1}^2 + \mathrm{Xl}_{M}^2}}\right)^T \tag{10}$$

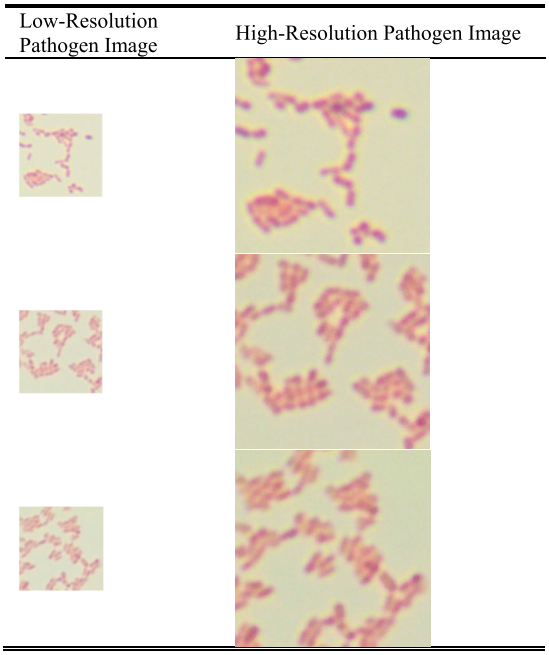

FIGURE 6. Result of super-resolution using ESRGAN.

TABLE 3. Classification results for different categories of pathogen using the basic CNN model.

Confusion Metric						
	Ai	Bp	Ca	Cp	Ei	Fm
Ai	215	0	3	0	23	0
Bp	0	222	0	14	2	3
Ca	0	0	235	5	0	1
Cp	0	4	9	228	0	0
Ei	8	0	3	0	230	0
Fm	0	0	14	0	2	225

classification using this basic Convolutional Neural Network (CNN) based model are shown in Table 3. As shown in the table classification accuracy for Candida. Albicans is 89.64% which is better than the other five categories of pathogens. The overall accuracy of classification is 83.23%. The graphical representation of classification results is shown in Figure 7.

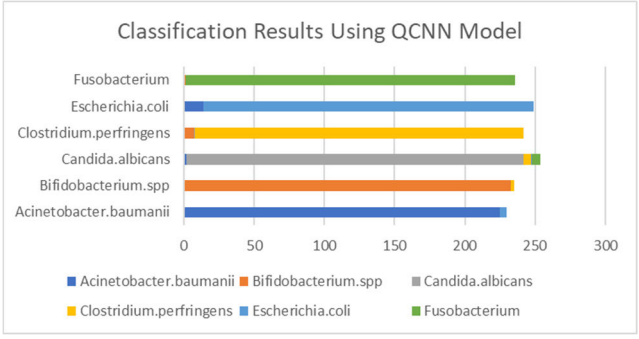

FIGURE 7. Graphical representation of classification results using the basic CNN model.

Then the images are tested using our proposed QCNN model. The results of pathogens classification are shown in Table 4 using the proposed QCNN model. The table shows the accuracy of classification for Candida. Albicans 99.9% which is better than the other five categories of pathogens. The overall accuracy of classification is 96.54%. The graphical representation of classification results is shown in Figure 8.

TABLE 4. Classification results for different categories of Pathogen using the QCNN model.

Confusion Metric						
	Ai	Bp	Ca	Cp	Ei	Fm
Ai	225	0	2	0	14	0
Bp	0	232	0	6	0	1
Ca	0	0	240	1	0	0
Cp	0	2	5	234	0	0
Ei	5	0	1	0	235	0
Fm	0	0	6	0	0	235

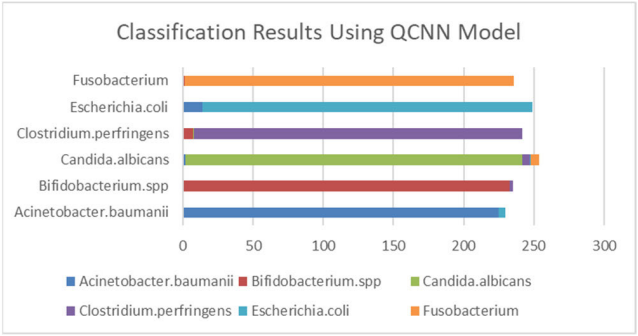

FIGURE 8. Graphical representation of classification results using the QCNN model.

the numerical evaluation of the classification results is performed using different performance measures such as accuracy, precision, recall, and F1 score. The values of performance measures are shown in Table 5 and their graphical representation is shown in Figure 9.

TABLE 5. Performance evaluation of the QCNN model.

Performance Measure	Value
Accuracy	96.54
Precision	93.6
Recall	92.8
F1 Score	92.5

For comparison purposes, results are also evaluated by applying pre-trained models (Alexnet, SSD Net, and FixNet) on the same dataset. In Table 6, the comparison of pre-trained models and QCNN models is presented, which shows that the QCNN model achieved better accuracy as compared to the original data. Results are taken out in terms of Accuracy, Precision, Recall, and F1 Score of each class. The trained model achieves an accuracy of up to 96.54% as shown in

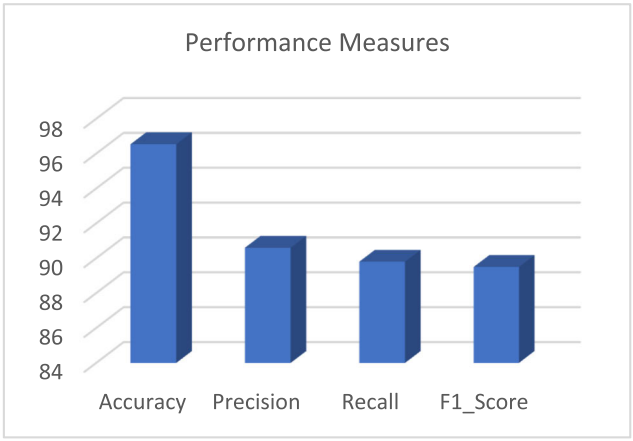

FIGURE 9. Graphical representation of the performance measures of the QCNN model.

TABLE 6. Results comparison for pre-trained and QCNN model.

Deep Features	Accuracy	Precision	Recall	F1 Score
Alexnet	0.64	0.62	0.47	0.54
SSD Net	0.86	0.68	0.89	0.77
FixNet	0.93	0.82	0.98	0.89
QCNN	0.96	0.93	0.92	0.93

TABLE 7. Comparative analysis of the proposed method with some existing techniques.

Ref.	Dataset	Types of Bacteria	Method	Acc
[52]	HOWMED, PIXNIO	Pathogenic bacteria species	CNN	95%
[53]	Digital microscopic images downloaded from Google	Vibrio cholera and plasmodium falciparum	CNN	94%
[54]	Dataset downloaded from the Kaggle website	Pathogenic bacteria	SVM	90.33%
[55]	Zebrafish dataset	Larval zebra fish intestinal bacteria	CNN	89.3%
[56]	ZN stained Sputum smear Images	Staphylococcus aureus and Lactobacillus delbrueckii	CNN	75%
[45]	Myxobacterial dataset	Myxobacteria	XGBoost	90.28%
[57]	Marine bacteria dataset	Marine bacteria	KNN	95%
Our	DiaBas	Pathogenic bacteria	QCNN	96.54%

Table 6. This problem is novel and there is no such method for detecting the bacteria in real-time from the water to check the contamination of water.

The comparative analysis of various methods for traffic sign classification is given in Table 7. The table shows that different authors have employed different methods for the classification task, including CNN, SVM, and XGBoost. Our proposed method utilizes the QCNN model. The accuracy is used to measure the performance of each method. Our proposed QCNN model achieves the highest accuracy of 96.54%, outperforming the other approaches.

V. CONCLUSION

A step-by-step pathogen classification algorithm has been proposed in this research work. Experimental results described in the result section demonstrate that the proposed system provides better classification accuracy on DIBAS databases. In the proposed work, the classification of six categories of the pathogen (Acinetobacter.baumanii, Bifidobacterium.spp, Candida.albicans, Clostridium. perfringens, Escherichia.coli, and Fusobacterium) is performed. QCNN Model was used and the quantum-based features of pathogens were utilized for the classification of these pathogen images in multiple categories for detecting the contamination of water. All the steps of the proposed algorithms are implemented in Python using an operating system of 64 bits with 16GB RAM, a 3.6GHz processor, and NVIDIA 4GB 1660 GTX. This method is effective and attains a classification accuracy of 96.54% on the pathogen database which is higher than the basic CNN classification model. The proposed method offers promising prospects for the future of bacterial classification with the potential for increased accuracy, precision, and sensitivity. The model can advance our understanding of pathogenic bacteria and their behavior. There were also some challenges which are faced during image acquisition and model training phase which are: a) Adding quantum layers to the neural network creates a lot of errors which takes a lot of time. b) Collection of datasets, Conversion of classical images into quantum images, extraction of quantum features, and hyper-parameter tunning was also a challenging task. This has implications for healthcare, enabling rapid and precise identification of bacteria for improved diagnostics and personalized treatment strategies. Furthermore, the utilization of quantum mechanisms stimulates technological innovation and interdisciplinary collaborations, pushing the boundaries of both quantum computing and microbiology. Overall, the model's future impact lies in its ability to enhance classification accuracy, provide novel insights, improve healthcare outcomes, and drive advancements in computational biology.

CONFLICT OF INTEREST

The authors declare that they have no conflicts of interest pertaining to the research presented in this manuscript.

REFERENCES

[1] S. Kotwal, P. Rani, T. Arif, J. Manhas, and S. Sharma, "Automated bacterial classifications using machine learning based computational techniques: Architectures, challenges and open research issues," *Arch. Comput. Methods Eng.*, vol. 29, no. 4, pp. 2469–2490, Jun. 2022.

[2] A. Soni, Y. Dixit, M. M. Reis, and G. Brightwell, "Hyperspectral imaging and machine learning in food microbiology: Developments and challenges in detection of bacterial, fungal, and viral contaminants," *Comprehensive Rev. Food Sci. Food Saf.*, vol. 21, no. 4, pp. 3717–3745, Jul. 2022.

[3] A. Paridon, A. Fox, and A. B. Alvero, "Detection of unfolded protein response by polymerase chain reaction," in *Detection of Cell Death Mechanisms*. New York, NY, USA: Humana, 2021, pp. 13–20.

[4] D. Kusić, B. Kampe, P. Rösch, and J. Popp, "Identification of water pathogens by Raman microspectroscopy," *Water Res.*, vol. 48, pp. 179–189, Jan. 2014.

[5] M. Hussain, Z. Chen, M. Lv, J. Xu, X. Dong, J. Zhao, S. Li, Y. Deng, N. He, Z. Li, and B. Liu, "Rapid and label-free classification of pathogens based on light scattering, reduced power spectral features and support vector machine," *Chin. Chem. Lett.*, vol. 31, no. 12, pp. 3163–3167, Dec. 2020.

[6] C. Osunla and A. Okoh, "Vibrio pathogens: A public health concern in rural water resources in sub-Saharan Africa," *Int. J. Environ. Res. Public Health*, vol. 14, no. 10, p. 1188, Oct. 2017.

[7] M. K. Osman, M. Y. Mashor, and H. Jaafar, "Detection of mycobacterium tuberculosis in Ziehl–Neelsen stained tissue images using Zernike moments and hybrid multilayered perceptron network," in *Proc. IEEE Int. Conf. Syst., Man Cybern.*, Oct. 2010, pp. 4049–4055.

[8] M. K. Osman, M. Y. Mashor, and H. Jaafar, "Performance comparison of clustering and thresholding algorithms for tuberculosis bacilli segmentation," in *Proc. Int. Conf. Comput., Inf. Telecommun. Syst. (CITS)*, May 2012, pp. 1–5.

[9] M. K. Osman, M. Y. Mashor, Z. Saad, and H. Jaafar, "Colour image segmentation of tuberculosis bacilli in Ziehl–Neelsen-stained tissue images using moving K-mean clustering procedure," in *Proc. 4th Asia Int. Conf. Math./Anal. Modelling Comput. Simulation*, May 2010, pp. 215–220.

[10] M. K. Osman, M. Y. Mashor, Z. Saad, and H. Jaafar, "Segmentation of tuberculosis bacilli in Ziehl–Neelsen-stained tissue images based on K-mean clustering procedure," in *Proc. Int. Conf. Intell. Adv. Syst.*, Jun. 2010, pp. 1–6.

[11] F. Ouertani, H. Amiri, J. Bettaib, R. Yazidi, and A. B. Salah, "Adaptive automatic segmentation of leishmaniasis parasite in indirect immunofluorescence images," in *Proc. 36th Annu. Int. Conf. IEEE Eng. Med. Biol. Soc.*, Aug. 2014, pp. 4731–4734.

[12] M. L. Chayadevi and G. T. Raju, "Data mining, classification, and clustering with morphological features of microbes," *Int. J. Comput. Appl.*, vol. 52, no. 4, pp. 1–5, Aug. 2012.

[13] R. Rulaningtyas, A. B. Suksmono, T. Mengko, and P. Saptawati, "Multi patch approach in K-means clustering method for color image segmentation in pulmonary tuberculosis identification," in *Proc. 4th Int. Conf. Instrum., Commun., Inf. Technol., Biomed. Eng. (ICICI-BME)*, Nov. 2015, pp. 75–78.

[14] K. S. Mithra and W. R. S. Emmanuel, "An efficient approach to sputum image segmentation using improved fuzzy local information C means clustering algorithm for tuberculosis diagnosis," in *Proc. Int. Conf. Inventive Comput. Informat. (ICICI)*, Nov. 2017, pp. 126–130.

[15] K. S. Mithra and W. R. S. Emmanuel, "Segmentation and classification of mycobacterium from Ziehl Neelsen stained sputum images for tuberculosis diagnosis," in *Proc. Int. Conf. Commun. Signal Process. (ICCSP)*, Apr. 2017, pp. 1672–1676.

[16] S. Andreatta, M. M. Wallinger, T. Posch, and R. Psenner, "Detection of subgroups from flow cytometry measurements of heterotrophic bacterioplankton by image analysis," *Cytometry*, vol. 44, no. 3, pp. 218–225, 2001.

[17] K. Milferstedt, M.-N. Pons, and E. Morgenroth, "Textural fingerprints: A comprehensive descriptor for biofilm structure development," *Biotechnol. Bioeng.*, vol. 100, no. 5, pp. 889–901, Aug. 2008.

[18] B. Vanhoutte, M. N. Pons, C. R. Thomas, L. Louvel, and H. Vivier, "Characterization of penicillium chrysogenum physiology in submerged cultures by color and monochrome image analysis," *Biotechnol. Bioeng.*, vol. 48, no. 1, pp. 1–11, Oct. 1995.

[19] J. Wang, R. Sarkar, A. Aziz, A. Vaccari, A. Gahlmann, and S. T. Acton, "Bact-3D: A level set segmentation approach for dense multi-layered 3D bacterial biofilms," in *Proc. IEEE Int. Conf. Image Process. (ICIP)*, Sep. 2017, pp. 330–334.

[20] Z. Zhou, M. N. Pons, L. Raskin, and J. L. Zilles, "Automated image analysis for quantitative fluorescence in situ hybridization with environmental samples," *Appl. Environ. Microbiol.*, vol. 73, no. 9, pp. 2956–2962, May 2007.

[21] C. Wählby, T. Riklin-Raviv, V. Ljosa, A. L. Conery, P. Golland, F. M. Ausubel, and A. E. Carpenter, "Resolving clustered worms via probabilistic shape models," in *Proc. IEEE Int. Symp. Biomed. Imaging*, Apr. 2010, pp. 552–555.

[22] S. Belkasim, G. Derado, R. Aznita, E. Gilbert, and H. O'Connell, "Multiresolution border segmentation for measuring spatial heterogeneity of mixed population biofilm bacteria," *Computerized Med. Imag. Graph.*, vol. 32, no. 1, pp. 11–16, Jan. 2008.

[23] W. Geng, P. Cosman, J.-H. Baek, C. Berry, and W. R. Schafer, "Image feature extraction and natural clustering of worm body shapes and motion characteristics," in *Proc. 5th IASTED Int. Conf. Signal Image Process.*, Aug. 2003, pp. 342–347.

[24] W. Geng, P. Cosman, J.-H. Baek, C. C. Berry, and W. R. Schafer, "Quantitative classification and natural clustering of caenorhabditis elegans behavioral phenotypes," *Genetics*, vol. 165, no. 3, pp. 1117–1126, Nov. 2003.

[25] H. Sajedi, F. Mohammadipanah, and H. K. S. Panahi, "An image analysis-aided method for redundancy reduction in differentiation of identical actinobacterial strains," *Future Microbiol.*, vol. 13, no. 3, pp. 313–329, Mar. 2018.

[26] L. Karthik, G. Kumar, T. Keswani, A. Bhattacharyya, S. S. Chandar, and K. V. B. Rao, "Protease inhibitors from marine actinobacteria as a potential source for antimalarial compound," *PLoS ONE*, vol. 9, no. 3, Mar. 2014, Art. no. e90972.

[27] B. A. Mohamed and H. M. Afify, "Automated classification of bacterial images extracted from digital microscope via bag of words model," in *Proc. 9th Cairo Int. Biomed. Eng. Conf. (CIBEC)*, Dec. 2018, pp. 86–89.

[28] D. Nie, E. A. Shank, and V. Jojic, "A deep framework for bacterial image segmentation and classification," in *Proc. 6th ACM Conf. Bioinf., Comput. Biol. Health Informat.*, Sep. 2015, pp. 306–314.

[29] L. Vanitha and A. R. Venmathi, "Classification of medical images using support vector machine," in *Proc. Int. Conf. Inf. Netw. Technol.*, vol. 4, 2011, pp. 63–67.

[30] A. Plichta, "Methods of classification of the genera and species of bacteria using decision tree," *J. Telecommun. Inf. Technol.*, vol. 4, no. 2019, pp. 74–82, Jan. 2020.

[31] V. Vijaykumar, "Classifying bacterial species using computer vision and machine learning," *Int. J. Comput. Appl.*, vol. 151, no. 8, pp. 23–26, Oct. 2016.

[32] A. Özmen and G. W. Weber, "RMARS: Robustification of multivariate adaptive regression spline under polyhedral uncertainty," *J. Comput. Appl. Math.*, vol. 259, pp. 914–924, Mar. 2014.

[33] G.-W. Weber, İ. Batmaz, G. Köksal, P. Taylan, and F. Yerlikaya-Özkurt, "CMARS: A new contribution to nonparametric regression with multivariate adaptive regression splines supported by continuous optimization," *Inverse Problems Sci. Eng.*, vol. 20, no. 3, pp. 371–400, Apr. 2012.

[34] A. Özmen, G.-W. Weber, Z. Çavuşoğlu, and Ö. Defterli, "The new robust conic GPLM method with an application to finance: Prediction of credit default," *J. Global Optim.*, vol. 56, no. 2, pp. 233–249, Jun. 2013.

[35] A. Özmen and G. W. Weber, "Robust conic generalized partial linear models using RCMARS method—A robustification of CGPLM," *AIP Conf. Proc.*, vol. 1499, no. 1, pp. 337–343, 2012.

[36] A. Özmen, G. W. Weber, İ. Batmaz, and E. Kropat, "RCMARS: Robustification of CMARS with different scenarios under polyhedral uncertainty set," *Commun. Nonlinear Sci. Numer. Simul.*, vol. 16, no. 12, pp. 4780–4787, Dec. 2011.

[37] Ö. F. Nasip and K. Zengin, "Deep learning based bacteria classification," in *Proc. 2nd Int. Symp. Multidisciplinary Stud. Innov. Technol. (ISMSIT)*, Oct. 2018, pp. 1–5.

[38] M. Talo, "An automated deep learning approach for bacterial image classification," 2019, *arXiv:1912.08765*.

[39] B. Zieliński, A. Plichta, K. Misztal, P. Spurek, M. Brzychczy-Włoch, and D. Ochońska, "Deep learning approach to bacterial colony classification," *PLoS ONE*, vol. 12, no. 9, Sep. 2017, Art. no. e0184554.

[40] L. Huang and T. Wu, "Novel neural network application for bacterial colony classification," *Theor. Biol. Med. Model.*, vol. 15, no. 1, p. 22, Dec. 2018.

[41] T. Ahmed, Md. F. Wahid, and Md. J. Hasan, "Combining deep convolutional neural network with support vector machine to classify microscopic bacteria images," in *Proc. Int. Conf. Electr., Comput. Commun. Eng. (ECCE)*, Feb. 2019, pp. 1–5.

[42] H. Wang, H. Ceylan Koydemir, Y. Qiu, B. Bai, Y. Zhang, Y. Jin, S. Tok, E. C. Yilmaz, E. Gumustekin, Y. Rivenson, and A. Ozcan, "Early detection and classification of live bacteria using time-lapse coherent imaging and deep learning," *Light, Sci. Appl.*, vol. 9, no. 1, pp. 1–17, Jul. 2020.

[43] V. Balagurusamy, V. Siu, A. D. Kumar, S. Dureja, J. Ligman, P. Kudva, M. Tong, and D. Dillenberger, "Detecting and discriminating between different types of bacteria with a low-cost smartphone based optical device and neural network models," *Proc. SPIE*, vol. 11087, Sep. 2019, Art. no. 110870E.
[44] C. You, Z. Li, M. Li, Z. Gao, and W. Li, "DB-Net: Dual attention network with bilinear pooling for fire-smoke image classification," *J. Phys., Conf. Ser.*, vol. 1631, no. 1, Sep. 2020, Art. no. 012054.
[45] H. Sajedi, F. Mohammadipanah, and A. Pashaei, "Image-processing based taxonomy analysis of bacterial macromorphology using machine-learning models," *Multimedia Tools Appl.*, vol. 79, no. 43, pp. 32711–32730, 2020.
[46] S. Lloyd, "Quantum machine learning for data classification," *Physics*, vol. 14, no. 44, p. 79, 2021.
[47] G. Sergioli, R. Giuntini, and H. Freytes, "A new quantum approach to binary classification," *PLoS ONE*, vol. 14, no. 5, May 2019, Art. no. e0216224.
[48] Z. Abohashima, M. Elhosen, E. H. Houssein, and W. M. Mohamed, "Classification with quantum machine learning: A survey," 2020, *arXiv:2006.12270*.
[49] V. Havlíček, A. D. Córcoles, K. Temme, A. W. Harrow, A. Kandala, J. M. Chow, and J. M. Gambetta, "Supervised learning with quantum-enhanced feature spaces," *Nature*, vol. 567, no. 7747, pp. 209–212, Mar. 2019.
[50] M. Schuld and N. Killoran, "Quantum machine learning in feature Hilbert spaces," *Phys. Rev. Lett.*, vol. 122, no. 4, Feb. 2019, Art. no. 040504.
[51] N. Moll, P. Barkoutsos, L. S. Bishop, J. M. Chow, A. Cross, D. J. Egger, S. Filipp, A. Fuhrer, J. M. Gambetta, M. Ganzhorn, A. Kandala, A. Mezzacapo, P. Müller, W. Riess, G. Salis, J. Smolin, I. Tavernelli, and K. Temme, "Quantum optimization using variational algorithms on near-term quantum devices," *Quantum Sci. Technol.*, vol. 3, no. 3, Jul. 2018, Art. no. 030503.
[52] Md. F. Wahid, T. Ahmed, and Md. A. Habib, "Classification of microscopic images of bacteria using deep convolutional neural network," in *Proc. 10th Int. Conf. Electr. Comput. Eng. (ICECE)*, Dec. 2018, pp. 217–220.
[53] B. B. Traore, B. Kamsu-Foguem, and F. Tangara, "Deep convolution neural network for image recognition," *Ecological Informat.*, vol. 48, pp. 257–268, Nov. 2018.
[54] N. Rahmayuna, D. S. Rahardwika, C. A. Sari, D. R. I. M. Setiadi, and E. H. Rachmawanto, "Pathogenic bacteria genus classification using support vector machine," in *Proc. Int. Seminar Res. Inf. Technol. Intell. Syst. (ISRITI)*, Nov. 2018, pp. 23–27.
[55] E. A. Hay and R. Parthasarathy, "Performance of convolutional neural networks for identification of bacteria in 3D microscopy datasets," *PLOS Comput. Biol.*, vol. 14, no. 12, Dec. 2018, Art. no. e1006628.
[56] T. Treebupachatsakul and S. Poomrittigul, "Bacteria classification using image processing and deep learning," in *Proc. 34th Int. Tech. Conf. Circuits/Syst., Comput. Commun. (ITC-CSCC)*, Jun. 2019, pp. 1–3.
[57] B. Liu, K. Liu, N. Wang, K. Ta, P. Liang, H. Yin, and B. Li, "Laser tweezers Raman spectroscopy combined with deep learning to classify marine bacteria," *Talanta*, vol. 244, Jul. 2022, Art. no. 123383.

ISRA NAZ received the M.S. degree in computer science from COMSATS University Islamabad, Wah Campus, Pakistan. Since 2018, she has been in the education field. She received the Institute Gold Medal and Campus Gold Medal from COMSATS University Islamabad, Wah Campus, for attaining top position in MCS. She is currently a Lecturer with the University of Wah, Wah Cantt, Pakistan. Her areas of specialization are automation and pattern recognition. She has publications in IF, SCI, and ISI journals and in national and international conferences. Her research interests include deep learning, algorithms design and analysis, machine learning, image processing, and big data.

JAMAL HUSSAIN SHAH received the Ph.D. degree in pattern recognition from the University of Science and Technology of China, Hefei, China. Since 2008, he has been in the education field. He is currently an Associate Professor with COMSATS University Islamabad, Wah Campus, Pakistan. His areas of specialization are automation and pattern recognition. He has 60 publications in IF, SCI, and ISI journals and in national and international conferences. His research interests include deep learning, algorithms design and analysis, machine learning, image processing, and big data.

MUHAMMAD HABIB UR REHMAN (Senior Member, IEEE) received the bachelor's and master's degrees from COMSATS University Islamabad, Pakistan, and the Ph.D. degree from the Faculty of Computer Science and Information Technology, University of Malaya, Malaysia. He is currently with the Center for Cyber-Physical Systems, Khalifa University of Science of Technology, United Arab Emirates, as a Postdoctoral Research Fellow. He is also working on trustworthy blockchain technologies for intelligent cyber-physical systems. He has been an Alumnae of DAAD's postdoctoral network, since September 2019. He has authored or coauthored 40 international publications, including journal articles, conference proceedings, book chapters, and magazine articles, whereby his four articles are categorized as highly cited publications by Web-of-Science. His research interests include blockchain technologies, cyber-physical systems, secure key management, big data, edge computing, the industrial IoT, the research and development of trust models for decentralized, and trustworthy artificial intelligence applications for cyber-physical systems. He is a Bright Spark Fellow. He received gold medals and 100% fee-waiver scholarships from the bachelor's and master's degrees from COMSATS University Islamabad.

MUHAMMAD RAFIQ (Member, IEEE) received the M.S. degree in electronics engineering from International Islamic University, Pakistan, in 2008, and the Ph.D. degree in information and communication engineering from Yeungnam University, Republic of Korea, in 2022. He is currently an Assistant Professor in game software with Keimyung University, Republic of Korea. He has extensive industry experience with a background in databases, business applications, and industrial technology solutions. His research interests include modern 3D game development, computer vision, and video description incorporating artificial intelligence and deep learning.

GYU SANG CHOI (Member, IEEE) received the Ph.D. degree in computer science and engineering from The Pennsylvania State University. He was a Research Staff Member with the Samsung Advanced Institute of Technology (SAIT), Samsung Electronics, from 2006 to 2009. Since 2009, he has been with Yeungnam University, where he is currently an Assistant Professor. His research interests include embedded systems, storage systems, parallel and distributed computing, supercomputing, cluster-based web servers, and data centers. He is also working on embedded systems and storage systems, while his prior research has been mainly focused on improving the performance of clusters. He is a member of the ACM.